Published in final edited form as:
Biochemistry. 2009 October 13; 48(40): 9471–9481. doi:10.1021/bi901034r.

Chloroquine Transport in *Plasmodium falciparum* I: Influx and Efflux Kinetics for Live Trophozoite Parasites using a Novel Fluorescent Chloroquine Probe

Mynthia Cabrera[‡], **Jayakumar Natarajan**[‡], **Michelle F. Paguio**[‡], **Christian Wolf**[‡,⊥], **Jeffrey S. Urbach**[‖], and **Paul D. Roepe**[‡,§,‖,⊥,*]

[‡]Department of Chemistry, Georgetown University, 37th and O Streets, NW, Washington, DC 20057

[§]Department of Biochemistry and Cellular & Molecular Biology, Georgetown University, 37th and O Streets, NW, Washington, DC 20057

[‖]Department of Physics, Georgetown University, 37th and O Streets, NW, Washington, DC 20057

[⊥]Center for Infectious Diseases, Georgetown University, 37th and O Streets, NW, Washington, DC 20057

Abstract

Several models for how amino acid substitutions in the *Plasmodium falciparum* Chloroquine Resistance Transporter (PfCRT) confer resistance to chloroquine (CQ) and other antimalarial drugs have been proposed. Distinguishing between these models requires detailed analysis of high resolution CQ transport data that is unfortunately impossible to obtain with traditional radio–tracer methods. Thus, we have designed and synthesized fluorescent CQ analogues for drug transport studies. One probe places a NBD (6–(N–(7–nitrobenz–2–oxa–1,3–diazol–4–yl)amino)hexanoate acid) group at the tertiary aliphatic N of CQ, via a flexible 6 C amide linker. This probe localizes to the malarial parasite digestive vacuole (DV) during initial perfusion under physiologic conditions and exhibits similar pharmacology relative to CQ, vs. both CQ sensitive (CQS) and resistant (CQR) parasites. Using live, synchronized intraerythrocytic parasites under continuous perfusion we define NBD-CQ influx and efflux kinetics for CQS vs. CQR parasites. Since this fluorescence approach provides data at much higher kinetic resolution relative to fast–filtration methods using ^{3}H–CQ, rate constants vs. linear initial rates for CQ probe flux can be analyzed in detail. Importantly, we find CQR parasites have a decreased rate constant for CQ influx into the DV, and that this is due to mutation of PfCRT. Analysis of zero trans efflux for CQS and CQR parasites suggests distinguishing between bound vs. free pools of intra-DV drug probe is essential for proper kinetic analysis of efflux. The accompanying paper [Paguio *et al.*, (2009), XXXX-XXXX] further probes efflux kinetics for proteoliposomes containing purified, reconstituted PfCRT.

Chloroquine (CQ) [1] and other quinoline drugs have been mainstays of malaria treatment for decades, but chloroquine resistance (CQR) in the malarial parasite *P. falciparum* is now a massive global problem. Design of effective second line therapies depends crucially on elucidation of the molecular mechanism(s) of CQR. Mutations in a unique digestive vacuolar (DV) polytopic integral membrane protein named *P. falciparum* Chloroquine Resistance

*Address correspondence to PDR: Tel 202 687 7300; Fax 202 687 6209; roepep@georgetown.edu.

SUPPORTING INFORMATION AVAILABLE

Supplemental data contains synthetic methods, characterization, and purification of NBD-CQ and intermediates. Also included are the fluorescence spectrum and thin-layer calibration of NBD-CQ. This material is available free of charge via the Internet at http://pubs.acs.org/.

Transporter (PfCRT) confer CQR in *P. falciparum* [1] but the molecular mechanism is not fully defined.

Decreased cellular accumulation of CQ is a well known characteristic of CQR parasites. Studies with live cells over the past 20 years report a variety of data and, in sum, the thermodynamic and kinetic characteristics of this phenomenon have not been elucidated. This is because historically the primary tool for such analysis has been filtration of parasite samples pre-incubated with radio-labeled drug at different time points, which does not provide data at high resolution. Yet, it is the precise definition of the kinetics and thermodynamics of CQ transport that is essential for distinguishing between various mechanistic proposals. These include that mutant PfCRT may mediate either active outward [2,3] or downhill passive [4,5] CQ transport across the DV membrane under certain conditions.

Coy Fitch was the first to measure reduced cellular accumulation of CQ linked to CQR in studies with an intrinsically drug resistant bird malaria [6]. Subsequently, the phenomenon of lower CQ accumulation for live CQR vs. chloroquine sensitive (CQS) parasites was carefully documented in other *Plasmodia* species, including the lethal human pathogen *P. falciparum* [1–3,5–15]. In reviewing these studies, it is difficult to consolidate much of the data and reconcile conflicting conclusions since many different methods and experimental conditions were employed. Key transport assay conditions (e.g. hematocrit, parasite density [parasitemia], buffer conditions, whether the parasite culture is synchronized vs. asynchronous, etc.) have varied considerably. In most experiments the conditions are non-physiologic since exogenous buffers and other variables must be manipulated to perform the measurements with conventional radio-tracer methods. Other key differences are the external concentrations of probe CQ (typically ^{3}H–labeled CQ) used for accumulation experiments, and the application of different mathematical approaches for estimating how much CQ within infected red blood cells (iRBC) is in the red cell vs. parasite localized, or how much represents saturable vs. nonsaturable uptake. It is exceedingly difficult to measure how much accumulated drug is free vs. bound to CQ target(s), however, Bray *et al.* have quantified CQ binding capacity under various conditions and concluded this can be 10 – 50 μM depending on conditions [16].

Accumulation differences for CQR vs. CQS parasites vary widely across previous studies. Importantly, Fitch and others have reported that the fold difference in accumulation of CQ for CQS vs. CQR parasites is strongly related to the external [CQ] used during the measurement. At higher external [CQ] (≥ 200 nM) the fold decrease in net cellular CQ accumulation is typically 2 fold or less for a CQR derivative relative to CQS, whereas at lower [CQ] differences ≥ 10 fold are sometimes calculated after subtraction of computed nonsaturable uptake. Variance in these previously measured differences might be due to depletion of external CQ during some experiments because it is low (1–2 nM) and the experiment is often done in a small fixed volume. Ambiguities could be further exacerbated by use of asynchronous culture and differences in cell cycle kinetics for CQS vs. CQR parasites, since different stages of the parasite accumulate different levels of drug. Presumably because accumulation differences for CQR vs. CQS parasites are larger at 1–2 nM CQ, and thus easier to quantify with bulk culture and radio-tracer methods, studies in this range of concentrations have been emphasized. More importantly however, plasma levels of CQ are much higher (to several μM) and *in vitro* 50% CQ inhibitory concentration (IC_{50}) for CQS and CQR parasites are 20–350 nM (in cytostasis assays) or 0.25–2.00 μM (in cytotoxicity assays) [17]. The expense of radio-labeled CQ and

[1]**Abbreviations**: CQ, chloroquine; CQR, chloroquine resistant; DV, digestive vacuole; PfCRT, *Plasmodium falciparum* chloroquine resistance transporter; CQS, chloroquine sensitive; iRBC, infected red blood cell; NBD-CQ, 6-(7-Nitro-benzo[1,2,5]oxadiazol-4-ylamino)-hexanoic acid (2-{[4-(7-chloro-quinolin-4-ylamino)-pentyl]-ethyl-amino}-ethyl)-amide; PL, proteoliposomes; HBSS, Hank's balanced salt solution; RBC, red blood cells; SCP, single cell photometry; ROI, region of interest; VPL, verapamil; SDCM, spinning disk confocal microscopy; AzBCQ, azido–biotin CQ; ATP, adenosine 5'-triphosphate; ΔpH, pH gradient; PfMDR1, *P. falciparum* multidrug resistance protein; HBS, HEPES buffered saline solution.

P. falciparum cell culture, as well as the very time consuming nature of traditional filtration approaches for assaying transport has presumably inhibited analysis of accumulation at this much wider range of CQ concentrations.

In this paper, we report on the synthesis and initial use of a valid fluorescent probe for cellular CQ transport, NBD–CQ. Pharmacology and subcellular localization of the probe is similar to CQ, and we find that differences in fold accumulation of NBD–CQ for CQR vs. CQS parasites are similar to what has been reported in many previous studies using ^{3}H-CQ and filtration methods. These results validate use of the probe to characterize influx and efflux kinetics, which we now define at enormously improved resolution for live, single cells. Importantly, unlike all previous CQ transport experiments of which we are aware, we analyze transport while cells are under constant perfusion with physiologically buffered media. We quantify levels of drug accumulation under constant perfusion as well as initial rates and rate constants for NBD–CQ influx and efflux. In the accompanying paper [18], we address the specific role that mutant PfCRT plays in these phenomena by purifying the protein, reconstituting it into proteoliposomes (PL), and devising NBD–CQ flux assays for rapidly mixed PL suspensions.

MATERIALS AND METHODS

Materials

P. falciparum strains Dd2 and HB3 were obtained from the Malaria Research and Reference Reagent Resource Center (Manassas, VA). Off-the-clot, heat-inactivated pooled O+ human serum and O+ human whole blood were purchased from Biochemed Services (Winchester, VA). SYBR Green I was purchased from Invitrogen Corporation (Carlsbad, CA). 100% CO_2 and custom 5% O_2/ 5% CO_2/ 90% N_2 gas blends were purchased from Robert's Oxygen (Rockville, MD). Hemin was purchased from Sigma-Aldrich (St. Louis, MO). Poly-L-lysine, RPMI 1640, hypoxanthine, Hanks Balanced Salt Solution Modified (HBSS) and Giemsa were from Sigma-Aldrich (St. Louis, MO). All other chemicals were reagent grade or better and purchased from commercial sources.

Methods

Cell Culture—All *P. falciparum* strains were maintained using the method of Trager and Jensen [19] with minor modifications. Fresh cultures are initiated from frozen vials containing glycerolyte and > 5% parasitemia kept in liquid N_2. Once active for at least two RBC cycles, cultures were maintained at 2% hematocrit in RPMI 1640 supplemented with 10% O+ human serum, 25 mM HEPES pH 7.4, 24 mM $NaHCO_3$, 11 mM glucose, 0.75 mM hypoxanthine, and 20 μg/l gentamycin. Parasitemia was monitored by Giemsa staining and set to 2% every 48 h. For experiments, hematocrit was cut to 1% and parasitemia set to ≥ 5%. Synchronized late trophozoite stage parasites were used in the perfusion experiments.

Synchronization—All cultures were routinely synchronized three times per cycle by 5% D-sorbitol treatment to obtain rings and some early trophozoites as described [20].

Antimalarial Drug Activity—Antimalarial drug activity was determined using the SYBR Green I method [21] with some modifications. Synchronous ring stage parasites at 5–10% parasitemia and 2% hematocrit were used as stock cultures. In brief, 100 μl of varying concentrations of NBD-CQ and CQ were prepared as 2 × concentrations in phenol-red free RPMI 1640 and plated in 96 well plates. Parasite cultures of equal volume were added to the drugs such that the levels of parasitemia and hematocrit at final dilution were 0.5% and 1.0%, respectively. The plates are placed in a sealed modular chamber, gassed with 5% O_2/ 5% CO_2/ 90% N_2 gas blend, and left at 37 ºC for 72 h. Standard curves were generated on the day the fluorescence measurements are done, using samples of known parasitemia [21].

Synthesis of NBD-CQ derivative—Following a literature procedure, [22] we prepared *N*-t-Boc-glycinal **3** in 90% yield from commercially available Weinreb amide **2** (c.f. Scheme 1). Reductive amination of **3** with monodesethyl chloroquine **4** in the presence of sodium cyanoborohydride produced 65% of carbamate **5**. Removal of the carbamoyl protecting group with 2M HCl gave primary amine **6** in 78% yield. Coupling of this CQ analogue **6** with commercially available succinimidyl 6-(*N*-(7-nitrobenz-2-oxa-1,3-diazol-4-yl)amino) hexanoate **7** furnished NBD-CQ derivative **1** in 85% yield. Supplementary information (NMR, HPLC, fluorescence spectra) is available free of charge at http://pubs.acs.org/.

Fluorescence Measurements—Fluorescence measurements were done at 37 ºC in rapidly mixed, jacketed 3 ml methacrylate cuvettes using a PTI Alphascan Fluorometer (Birmingham, NJ). Excitation and emission wavelengths, etc. are described in the relevant captions.

Preparation of Samples for Microscopy—200 µl of 1% hematocrit culture of late stage trophozoite parasites was pelleted by centrifugation and resuspended in 400 µl of culture media without serum. In general, 200 µl of resuspended cells were placed on poly-L-lysine coated coverslips and incubated for 3 min under standard cell culture atmosphere. Non-adherent cells were washed off and the coverslip was mounted on custom-designed perfusion chambers for SDCM or SCP as described in detail elsewhere [20,23–25].

Single Cell Photometry (SCP)—SCP was via methods described in detail elsewhere [23, 24]. The apparatus essentially consists of a custom-built Nikon Diaphot epifluorescence microscope with a 100x fluor objective, an attached 8-bit COHU CCD camera, and a computer controlled xenon arc lamp. Lamp illumination is controlled by our custom software to set both wavelength and to completely block illumination between data acquisition steps (typically 3 sec recovery time between 100 msec illumination steps). Excitation was filtered using a 460 nm band pass filter (10 nm width) and emission collected with 535 nm long pass filter attached to a 515 nm dichroic mirror. On-chip integration times varied depending on the dynamic thresholding set by the software, which also constantly corrects for background within 1–2 µm of a “donut” region of interest (ROI) [see 23]. Intracellular NBD-CQ concentrations were computed using thin-layer calibration at known concentrations as described [24], for NBD-CQ trapped within RBC (see Results). NBD-CQ fluorescence at fixed concentrations of hematin was also measured by thin layer calibration as described [24].

Parasites were always maintained under constant perfusion at 3 ml/min of a physiologic buffer, HBSS, with 5% O_2 and 5% CO_2 (balance N_2) and at 37 ºC as described [20,23,24]. Parasites were initially perfused for 5 min with gas balanced HBSS, and then with known concentrations of NBD-CQ in the same physiologic buffer. Efflux was typically initiated by perfusion with HBSS without NBD-CQ after probe accumulation reached plateau.

Rates of influx and efflux were calculated by curve-fitting using SigmaPlot 9.0 software. Accumulation rate constants were obtained by fitting influx to $f = y_o + a(1\text{-}e^{(-bx)})$. Efflux rate constants were obtained by fitting efflux trace to $f = y_o + ae^{-bx}$. Initial rates were calculated by fitting to $y = mx + b$. Glucose starvation was by perfusion with gas balanced HBSS containing 2 mM 2-deoxy-D-glucose instead of 5 mM glucose, for 15 min as described [25] or by perfusion without any glucose substitution. Influx of 250 nM NBD-CQ in glucose free HBSS was measured for 15 min and efflux under glucose deprived conditions was measured by immediately changing to glucose free HBSS without NBD-CQ at the end of the 15 min accumulation.

For influx measurements in the presence of 1 µM verapamil (VPL), cells were perfused with gas balanced HBSS for 5 min, HBSS plus 1 µM VPL for another 5 min, then HBSS with 250 nM NBD-CQ and 1 µM VPL for 15 min more.

Very low external NBD-CQ—To mimic some previous experiments done with ^{3}H–CQ, NBD–CQ accumulation was also measured in iRBCs after 60 min of incubation with 1 nM NBD–CQ in HBS pH 7.4 under culture conditions. In this case, NBD–CQ was allowed to accumulate in parasite cultures with 1% hematocrit and 5% parasitemia, cells were attached to coverslips as above, and DV localized NBD–CQ quantified by imaging many different ROIs for several coverslips (see Results). Parallel experiments were done with ^{3}H–CQ to measure cellular accumulation essentially as described [9].

Spinning Disk Confocal Microscopy (SDCM)—The SDCM apparatus used is as described in detail elsewhere [17,20,25] with some modifications. The camera was an Andor iXon DV887 back illuminated EMCCD, and for fluorescence SDCM, excitation was with a Coherent Innova 300 I Ar/Kr Laser (488 nm) and exposure time was 100 ms with z-spacing of 200 nm.

RESULTS

Elucidating cellular transport kinetics for a drug (e.g. CQ) by use of a chemically modified probe (e.g. a fluorescent CQ derivative such as NBD-CQ) could in theory be complicated by changes in the drug's physical properties caused by the derivatization. A valid probe should behave similarly to underivatized CQ. Our definition of a valid probe for analysis of physiologically relevant CQ transport is: 1) relative sensitivity (IC_{50}) of the compound and fold difference in that sensitivity for CQR vs. CQS malarial parasites should be similar to that seen for CQ; 2) subcellular localization of the probe is (best one can ascertain) identical to that previously found for ^{3}H–CQ via *in situ* autoradiography [26]; and 3) relative steady state accumulation of the probe is reduced for well defined laboratory strains of CQR parasites relative to CQS, and to a similar extent when compared to previous ^{3}H–CQ/fast filtration data. As described below, one probe we have created (NBD–CQ) satisfies these criteria.

NBD–CQ was synthesized from monodesethyl CQ and a commercially available fluorophore tag as described in Methods and Scheme 1. Characterization and purification of the probe are shown in Supplemental Information (Fig. S1–S3). Because CQ can tolerate multiple side chain modifications without loss of activity, and since tags placed at the ethyl group termini of CQ did not appear to perturb physiologically relevant binding of CQ to PfCRT protein [27], the NBD fluorophore was attached to the CQ side chain terminus via a similar strategy reported earlier for AzBCQ [27]. This placement does not perturb CQ pK_a essential for parasite vacuolar localization (see below) and leaves the 7-chloro-4-amino pharmacophore that defines binding to free heme [28] fully intact. Excitation and emission spectra of the highly fluorescent probe as well as linear intensity vs. concentration plots under both bulk and thin layer (i.e. SCP; see [23]) conditions may be found in Supplemental Information (Fig. S4).

Toxicity of NBD–CQ was quantified for CQS (strain HB3) and CQR (strain Dd2) malarial parasites using the SYBR–green assay [21] and IC_{50} found to be 26 (± 9) nM and 184 (±18) nM respectively. Although the SYBR-green assay is fluorescence-based and some competition between NBD-CQ and SYBR-green fluorescence is in theory possible, control wells with 0.1 – 0.5 μM levels of NBD-CQ alone and various NBD-CQ / SYBR-green mixtures showed fluorescence of the drug probe at these concentrations was irrelevant vs. that of SYBR-green and did not affect calculation of IC_{50} (not shown). Previous quantification of CQ IC_{50} for these strains in our laboratory and others range from 10–30 nM and 120–200 nM respectively, and in our hands are 15 (±4) nM and 155 (±12) nM using the same SYBR-green assay. So although precise IC_{50} values for NBD–CQ are not exactly the same as for CQ, they fall within the range reported for CQ by a number of laboratories. More importantly, CQR parasite resistance to NBD–CQ is similar to CQ.

Fig. 1 shows that NBD–CQ localizes to the parasite digestive vacuole (DV) under live cell perfusion conditions used in this work, for both HB3 CQS parasites (A, C, E, G) and Dd2 CQR (B, D, F, H) (see Fig. caption and Methods). Importantly, we show that adenosine 5'-triphosphate (ATP) depletion (C, D, E, F) and VPL treatment (G, H) do not affect DV localization of quinoline under initial perfusion conditions for either CQS or CQR parasites. Although other cellular targets for CQ most likely exist [17], and although relative toxicity of the interactions with these different targets is not yet understood, the DV is believed to be the principle site of initial CQ accumulation and also the site of a principle CQ target, namely, heme released from hemoglobin digestion (e.g. [5,26,28]). The only other previously published parasite subcellular localization data for a quinoline drug of which we are aware reports approximately 1 nM external ^{3}H–CQ localization via *in situ* autoradiography, and shows that this is DV specific (Fig. 1 in ref [26]). Taken together then, initial pharmacology and subcellular localization results show that NBD–CQ is a valid probe for measuring CQ accumulation within live malarial parasites.

Previously, we constructed single cell photometry (SCP) systems that are optimized for quantifying small changes in intracellular fluorescence intensity vs. time [23,24]. These SCP methods are easily adapted to monitor the increase in probe fluorescence (DV NBD-CQ concentration) vs. time while iRBC are under perfusion with physiologic solution harboring low levels of NBD–CQ. To quantify the levels of NBD–CQ accumulated within the DV, we first generated calibration curves using various [NBD–CQ] equilibrated within uninfected RBC. The RBC were previously treated with protonophore to collapse any pH gradient (ΔpH) across the plasma membrane, such that incubating concentrations of NBD–CQ were then equal to internal (representative calibration curves can be found in Fig. S5). These equilibrated RBC harboring variable [NBD–CQ] were then imaged with the same SCP instrument under identical conditions. NBD–CQ intensities were measured and averaged across many RBC, and average intensities then plotted vs. known [NBD–CQ]. Two calibration curves were routinely generated (at pH 5.2 and 5.6) since, although the point remains somewhat controversial [29–31], we favor the interpretation that the DV pH is near 5.2 for Dd2 CQR parasites and nearer 5.6 for HB3 CQS [23,32,33]. Regardless, calibration at 5.2 vs. 5.6 does not differ under thin layer calibration conditions (see Fig. S5) thus conclusions related to the kinetics of NBD–CQ transport for these CQS vs. CQR parasites are not dependent on very small calibration differences at pH 5.2 vs. 5.6 (see Discussion). Free heme released from hemoglobin digestion within the DV could also conceivably affect the magnitude of DV NBD–CQ fluorescence. Best available estimates for free heme within the DV based on rates of hemoglobin digestion give an upper limit of < 1 μM [20], but these are clearly overestimates, due to low DV pH and heme solubility limits at these pH [34]. Thin layer NBD–CQ calibration curves at different pH +/− μM concentrations of heme show < 10 % quenching when the ratio of heme : NBD – CQ is < 0.2, as must be the case for the experiments described here, and quenching ~30% when heme : NBD – CQ is 1 (Fig. 2). These issues are explored further in Discussion.

With these caveats in mind we tested whether measured accumulation of NBD–CQ via our SCP methods is similar to that of cellular ^{3}H–CQ measured with previous filtration methods. Thus a traditional tube–based assay followed by fast filtration of ^{3}H–CQ loaded iRBC at different times was compared to similar tube–based accumulation of NBD–CQ, that was then quantified by microscopy using calibration curves described above. In this analysis we do not subtract computed theoretical "non saturable" uptake to calculate "saturable", rather, we compare raw (unprocessed) uptake data for identical cultures. Fig. 3 shows that accumulation of ^{3}H–CQ vs. NBD–CQ does not differ significantly after 60 min of incubation. Both CQS (HB3, left side) and CQR (Dd2, right) parasites accumulate 1 nM ^{3}H–CQ to levels reported many times previously, and Dd2 parasites show a similarly reduced level of either ^{3}H–CQ or NBD–CQ relative to HB3.

The sensitivity of our current SCP apparatus does not allow us to analyze NBD–CQ accumulation in real time at adequate signal–to–noise ratio for perfused live cells, when perfusate [NBD–CQ] is < 50 nM (not shown). However, at ≥ 50 nM concentrations single cell DV specific accumulation is easily resolved using SCP techniques previously developed in our laboratory. As expected (Fig. 4), reduced probe accumulation vs. time is found for Dd2 vs. HB3 parasites (Fig. 4, compare panel A vs. B), and reduced accumulation persists across a variety of fixed external [NBD–CQ] (see Table I), similar to data for CQ [9]. Importantly, unlike all previous work with radio-isotope probes, these accumulation traces are obtained in real time, with live intraerythrocytic parasites under continuous perfusion with physiologic perfusate. Measured differences in NBD–CQ accumulation for CQS vs. CQR parasites are not identical to some earlier static measurements with ^{3}H–CQ, but they are quite similar to several previous studies done at these concentrations (e.g. [9]). Note also that no subtraction of estimated “non saturable uptake” is performed for Fig. 3 and 4 or Table I. This operation heightens the fold difference that is often reported in other recent studies.

Since many data points are collected in digital form, linear initial rates and true rate constants for these accumulation traces are easily computed, and can be quickly averaged for many individual late stage trophozoites (note that we use only highly synchronized culture that is confirmed visually). Consistent with a reduced amplitude of accumulation (*c.f.* Fig. 4 A vs. B), we compute a reduced linear initial rate of NBD–CQ accumulation for CQR parasites relative to CQS (Fig. 4, D vs. C) either in the presence (open symbols D vs. C) or absence (closed symbols) of glucose. However, again consistent with previous studies, differences in initial rates for glucose starved CQR vs. CQS parasites are smaller than those measured in the presence of glucose. Interestingly, for the first time, we measure clearly reduced rate constants for NBD–CQ DV accumulation in CQR parasites relative to CQS at a range of NBD–CQ concentrations, when glucose remains constant in the perfusate (Fig. 4, F vs. E, open symbols). More intriguingly, this dramatic difference in rate constants is normalized when accumulation is measured in the absence of glucose (Fig. 4, F vs. E, closed symbols). A reduced linear initial rate of accumulation is a trivial prediction of a reduced amplitude (Fig. 4 A–D), and both observations could in theory be due to a decreased concentration of (or lowered affinity for) drug targets within the DV [4–7,14,16]. However, reduced rate constants derived from single exponential fits to these data indicates that net physical translocation of the probe across the DV membrane proceeds more slowly for CQR parasites relative to CQS. One possible explanation is that an ATP dependent uptake process that exists for CQS parasites is absent for CQR, and another is that net outward translocation of NBD–CQ for CQR parasites kinetically competes vs. ATP dependent probe accumulation.

To distinguish between these possibilities, we first compared HB3 (CQS) and Dd2 (CQR) parasites to CQS and CQR parasites created by transfection with mutant PfCRT (Table 2). Reduced accumulation, initial rate, and rate constant is seen for $C4^{Dd2}$ (CQR) transfectants vs. $C2^{GC03}$ (CQS, see [35]), similar to the trend noted for Dd2 vs. HB3. Since the two transfectant lines express the same isoform and levels of the *P. falciparum* multidrug resistance protein (PfMDR1) as well as other ATP dependent DV transporters, and since function of PfCRT protein is not directly ATP dependent, it seems unlikely that an ATP dependent DV membrane transporter that imports drug to CQS parasite DV is absent for CQR.

To further test the basis of pronounced differences in accumulation rate constants, we attempted to isolate differences in NBD–CQ efflux rate constants for CQS vs. CQR parasites. To manipulate the levels of probe preloaded into the DV we varied external incubating concentrations of NBD–CQ, and to examine possible differences in binding sites as proposed [16] we also varied time for the pre-incubation. Figure 5 shows that both incubation time and incubating concentration are critical in analysis of drug efflux from live parasites. That is, we first analyzed NBD–CQ efflux similar to how most previous studies have analyzed ^{3}H–CQ

efflux. Namely, when CQS (HB3, left) and CQR (Dd2, right) parasites are preloaded for 1 hr at nM levels of NBD–CQ, and then analyzed for NBD–CQ efflux in a volumetric excess of buffer (Fig. 5, top two traces, dashed lines) we find that Dd2 parasites release more preloaded drug probe relative to HB3 and also efflux the probe considerably faster. This is strikingly similar to many previous ^{3}H–CQ efflux measurements done via a similar approach. However, when we preload the parasites to the same internal [NBD-CQ] via very short term (1 minute) perfusion with 250 nM external NBD–CQ, initiate zero trans efflux by rapidly switching to perfusate without NBD–CQ (Fig. 5, bottom trace each panel, solid lines), and then continue to monitor efflux under constant perfusion, the traces for CQS and CQR parasites appear much more similar. These data clearly indicate that time dependent intracellular binding phenomena significantly complicate analysis of zero trans efflux kinetics.

To further explore DV efflux kinetics under conditions wherein complexities from time dependent binding are minimized, we varied incubating [NBD–CQ] in the perfusate but kept preloading times short (< 15 min). Fig. 6 shows representative efflux traces for CQS (HB3, left side) and CQR (Dd2, right side) parasites at higher intra-DV [NBD–CQ] (Fig 6, A, B) and also summarizes initial rates (Fig. 6, C, D) averaged from hundreds of experiments over a range of intra-DV probe concentrations.

To our knowledge, these are the first truly “zero trans” CQ efflux experiments for live malarial parasites, since they are acquired under constant perfusion with zero NBDCQ in the perfusate. Under these conditions, in contrast to data in Fig. 5 (top traces, each panel), initial rates of efflux either in the presence (open symbols) or absence (closed) of glucose are quite similar for CQS (Fig. 6, C) and CQR (D) parasites. Small differences are found at several concentrations, and linear curve fits to these data show small differences in slope (see caption).

To analyze efflux in more detail, rate constants were computed for these data (Fig. 7, A, B) as well as similar zero trans perfusion efflux data obtained after even shorter (1 min) pulse with NBD–CQ to preload the DV (Fig. 7, C, D). When rate constants are computed a small increase in efflux is seen for CQR parasites but only at lower DV concentrations of NBD–CQ (Fig. 7, B vs A), and the difference is not statistically significant (p-value= 0.55, see Discussion). However, as pre-incubation time is reduced further to 1 min (Fig. 7, C, D), we notice two important features. First, higher values for efflux rate constants are measured for both CQS and CQR parasites relative to rate constants computed for cells preloaded for longer time (note position of dashed lines). We suggest this is due to a higher percentage of DV entrapped probe being freely exchangeable (not bound) upon very short term pre-incubation. Second, slightly more dramatic increases in efflux rate constant are seen for CQR (D) vs CQS (C) parasites, again at lower DV concentrations. Again the differences are not statistically significant (p-value= 0.15, see Discussion), but comparing these data to Fig. 5 suggests to us that time dependent binding within the DV prevents unambiguous definition of differences in zero trans efflux rate constants for live cells.

DISCUSSION

Amphipathic hydrophobic drugs like CQ passively diffuse quickly across membranes, and live cells bind amphipathic drugs at intracellular binding sites. Thus, particularly in the presence of a drug gradient, it has proved exceedingly difficult if not impossible to kinetically characterize drug transport by putative drug transporters using live cells, radio-labeled drugs, and traditional fast filtration methods. Years of fast filtration of preloaded cells, vesicles, and PL preparations harboring PfCRT isoforms has convinced us that rigorous kinetic resolution of any PfCRT mediated drug transport ultimately requires alternate methodologies. Although fluorescent drug probes such as NBD–CQ are imperfect in the sense that they are not chemically identical to CQ, they are obviously far superior in terms of the ability to kinetically define

transport. After inspecting several fluorescent derivatives, NBD–CQ was found to have similar pharmacology and (best we can ascertain) identical subcellular localization relative to CQ. It was also found to be accumulated to lower levels for CQR parasites, similar to the behavior of CQ. We also note the fluorescent tag is added to the end of the flexible alkyl side chain via a flexible linker, a geometry for tag placement that does not appear to affect physiologic binding to a single drug binding site we have previously defined for PfCRT [27]. In the binding studies, a perfluoro azido group was placed in the same position as the NBD tag is placed in the present work. Specific inhibition of perfluoro azido CQ photolabelling is achieved at a remarkable 7–30 fold molar excess CQ, depending on the PfCRT isoform examined. This is exceedingly impressive competition that shows specificity for CQ–PfCRT interactions is not lost upon addition of tags at the end of the CQ alkyl side chain. Furthermore, a previous insightful paper [36] measured passive influx of CQ into RBC to derive a CQ permeability coefficient of ~ 2.00 cm/sec. Assuming permeability of the DV membrane is similar to that of the RBC plasma membrane, and correcting for differences in DV vs RBC membrane surface area [36], estimates a passive influx of CQ into the DV of ~ 150 CQ/DV/sec at 500 nM external CQ. We measure ~130 NBD-CQ/DV/sec (HB3 parasites) at 500 nM external NBD-CQ, indicating that the kinetics of NBD-CQ passive influx are very similar to those of CQ. For these reasons, we conclude that transport of NBD–CQ recapitulates the essential features of CQ transport.

Early on CQ transport was assessed in the μM range [6–9], presumably because peak plasma [CQ] for malaria patients is > 1 μM. Over the years, for whatever reasons, the practice of using μM range CQ concentrations for transport has shifted to using nM levels of drug. The greatest differences in uncorrected fold accumulation of CQ (meaning, accumulation data wherein estimated theoretical nonsaturable uptake has not been subtracted from total) for CQR vs. CQS parasites that have been reported are seen at [CQ] of 1 nM or less. These differences are typically 1.5 to 5 fold, depending on the conditions. However, we argue that 1 nM is well outside the therapeutic range of the drug, being an order of magnitude below typical growth inhibition IC_{50} for CQS parasites (10–30 nM) and at least 2 orders of magnitude below for CQR (125–350 nM). At 50–200 nM [CQ], fold differences in net accumulation have ranged from 50 % [7], 60 % [11], 2 fold [6], etc. In this study, we have examined a wide range of concentrations for live cells under continuous perfusion and have also been able to vary loading times prior to zero trans efflux measurements, without centrifugation and washing of cells, detergent extraction of iRBC parasites, or other potentially deleterious processing steps.

To our knowledge, no previous CQ accumulation or efflux experiments have been done with live intraerythrocytic parasites under perfusion using physiologically buffered perfusate (5% CO_2 / 5 % O_2 / 24.2 mM HCO_3^-). These are also the first data to our knowledge collected for individual ROI defined as individual DV within single parasites from highly synchronized culture. Along with vastly improved temporal resolution relative to traditional fast filtration approaches, that then allows definitive curve fitting, this makes the data in this paper unique. Perfusion conditions permit three important improvements for analysis of transport. First, analysis can be done under physiologic buffering (24.2 mM HCO_3^- and continuously replaced 5% CO_2). Since DV pH is regulated by these parameters and the DV membrane pH gradient is a principle driving force for initial accumulation of diprotic CQ (or diprotic NBD-CQ with identical pK_a), this is important. Second, accumulation is analyzed at a truly fixed external concentration, and truly zero trans efflux (constant zero external probe) can be measured. This is important for precise and accurate definition of influx and efflux kinetics, and is critical for quantitative comparison between parasite strains. Third, we are able to inspect a much wider variety of accumulation and preloading conditions prior to initiation of efflux under true zero trans conditions. This last improvement is also critical. All previous studies of which we are aware essentially present efflux data similar to what we show in Fig. 5 (top traces), but clearly this efflux behavior is only seen under certain preloading conditions.

Reduced amplitudes for uptake as well as lower initial rates of uptake (Fig. 4 A–D) have been observed in many previous studies of ^{3}H-CQ accumulation. In this paper, for the first time, we show that reduced net uptake for CQR parasites is also, at least in part, due to a reduced rate constant for accumulation. Importantly, rate constant varies vs. [NBD-CQ] for CQS parasites in the presence of ATP, but is linear for CQR. In the absence of ATP, the relationship is linear for both CQS and CQR. A linear relationship is diagnostic of transmembraneous passive diffusion whereas a hyperbolic shape (CQS+ATP) suggests some type of enzymatic or quasi enzymatic process.

Thus, the distinction between a reduced rate constant vs. reduced initial rate is very important. The former shows that the molecular process of transmembraneous movement inward is physically slower, whereas the latter could simply be due to reduced intracellular drug binding. If viewed only alongside the top traces shown in Fig. 5 it would be tempting to speculate that the significant decrease in accumulation rate constant for CQR parasites is due to a robust outward transport process, specific to CQR parasites, that kinetically competes with influx. However, efflux data obtained in this fashion clearly overestimates any contribution of an outward directed transport process to lowered net accumulation. Comparing parasites preloaded to the same levels of DV probe, but in one case loaded at low external levels for long time (60 min), and in the other, higher levels for very short time (1 min) clearly demonstrates time dependent binding to intracellular targets that differs for CQS vs. CQR parasites, and begins to quantify the magnitude of this effect. Similar observations have been made with ^{3}H-CQ, but at much lower kinetic resolution, by Bray, Ward and colleagues [16]. It has not been possible (until now) to preload for ~ 1 minute time periods, because transport has been assessed with bulk populations of cells that require centrifugation, washes, etc. But, under fast perfusion, and using single cell methods, preincubation conditions (time, [probe], etc.) can be varied and controlled much more easily. Thus, we are now able to provide evidence that under conditions where binding differences are minimized by very short term incubation, zero trans efflux kinetics are actually much more similar than data presented in Fig. 5 (top traces, each panel) would imply. We do find a small increase in the rate constant for efflux from CQR parasites at lower levels of DV probe, but with live cells and these methods the increase is not statistically significant (at ~ 3.5 μM internal NBD-CQ, p value = 0.55). That increase appears to become more dramatic as incubation times are shortened (hence time dependent binding is further reduced), but again the increase is not statistically significant (at ~ 3.5 μM, p value = 0.15). Perhaps more importantly, efflux rate constants are found to be faster than influx rate constants for both CQS and CQR parasites, suggesting either that a process other than passive transmembraneous diffusion is rate limiting for influx, or, that an efflux process faster than inward passive diffusion exists for *both* CQS and CQR parasites. It is also of course possible that both are relevant.

As described below and in the following paper [18] these data are suggestive of an outward directed drug efflux process that exists for CQR parasites, mediated by PfCRT. However, combined with inspection of Fig. 5, they lead us to suggest that some combination of altered intra DV binding, reduced ATP dependent uptake, and increased efflux is responsible for net decreased cellular accumulation of CQ in CQR parasites. Quantification of the relative importance of each contributing factor requires additional approaches, as described in the accompanying paper [18].

That is, from our inspection of these data, it seems unlikely that the very small increase in rate constant for CQR parasite efflux that perhaps exists can fully explain the much more significant decrease in accumulation rate constant for CQR parasites relative to CQS. In comparing these rate constant effects, it seems more likely to us that multiple effects must be adding together, only one of which would be heightened efflux. We propose that the lower accumulation rate constant for Dd2 vs. HB3 is also due in part to a DV accumulation process that is normally

present in HB3 that becomes impaired in Dd2. This process is directly or indirectly ATP dependent, since upon glucose starvation the accumulation rate constants normalize. Perhaps not coincidentally, this normalization occurs concomitant with collapse of the DV membrane pH gradient (see [25]), suggesting it is DV pH or ΔpH dependent. Four possibilities for this perturbed influx process are immediately obvious: 1) ATP dependent influx of quinoline directly catalyzed by the PfMDR1 protein situated in the DV membrane that is different for CQS vs. CQR parasites due to mutations in PfMDR1, 2) pH gradient dependent influx of quinoline directly catalyzed by the CQS isoform of PfCRT [but not the CQR isoform], 3) ATP (intra DV pH) dependent binding of quinoline to DV binding sites, 4) indirectly ATP dependent (meaning, ΔpH or membrane potential dependent) drug efflux via CQR isoform PfCRT that kinetically competes with uptake into CQS parasites. Possibilities 1, 3 and 4 (but not 2) have been examined in this paper. The data does not formally distinguish between possibilities 2, 3 and 4, but does eliminate possibility 1, since the $C4^{Dd2}$ and $C2^{GCO3}$ transfectants express similar levels of the same PfMDR1 isoform (both transfectants are derived from the same strain GCO3 parent and were created without any CQ selection pressure). Those data also suggest, but do not prove, that possibility 4 may play a role, but if so, it likely does not fully explain the change in influx rate constants for CQR parasites. Hence again, along with considering data in Fig. 5, we conclude that possibility 3 makes an important contribution to overall reduced net accumulation. These concepts are explored further in the accompanying paper [18].

A possible limitation to our methodology is NBD–CQ quenching that might exist, particularly quenching due to various chemical forms of non-crystallized heme within the DV. If appreciable free heme is present but the levels of heme are the same for CQS and CQR parasites, then our calculations for DV concentrations (mol probe per DV) and transport kinetics (mol probe per DV per sec) are somewhat inaccurate, but kinetic comparison of the rate constants between the two strains is empirically precise. If concentrations of free heme differ, then in theory differences in amplitudes and influx kinetics we observe could actually be slightly larger, and the statistically insignificant difference in efflux rate constants could also actually be larger. This is in fact likely to be the case to some extent because free heme is likely 2–fold lower in concentration for CQR DV relative to CQS. This is because volume of this organelle increases 2 fold for CQR parasites [25] but the same amount of hemozoin is produced in similar time [20]. So any heme–mediated quenching of NBD–CQ, even if only minor, would lead to slight under estimation of NBD–CQ levels found in HB3 DV, relative to those found in Dd2 DV. If that were indeed the case, the small increases in rate constant of efflux for CQR parasites that we find may be slightly underestimated. We believe this issue is also resolved in the accompanying paper [18].

Based on extensive analysis of ^{3}H–CQ accumulation data, Bray, Ward and co-workers have hypothesized that DV binding of CQ is reduced for CQR vs. CQS parasites [16]. Via this model, the level of accumulation vs. time should be reduced for CQR parasites, and the initial rate of accumulation would be reduced as a simple consequence. This would not perturb rate constants as we now report, but would explain the observations summarized in Fig. 5. Integrating the Bray and Ward heme binding model into what has been learned more recently regarding heme–CQ interactions [37,38] leads us to suggest that interconversion of heme pools from forms that do not bind drug to those that do (for example, phase partitioning of heme from lipid to aqueous environment within the DV [38] along with drug induced perturbation of heme monomer : dimer ratios [37]) might be rate limiting for some portion of drug uptake and could even be cooperative. These possibilities merit additional study.

In sum, we present the first definition of significantly reduced quinoline accumulation rate constants for the DV of CQR parasites relative to CQS. We propose that this is due to the sum of at least two processes, one of which is ATP (DV pH) dependent binding, the other being CQR isoform PfCRT-mediated outward efflux. But with regard to the latter, the data in this

paper are statistically inconclusive and do not define the thermodynamics or kinetics of that process. Such definition requires purification, reconstitution, and detailed analysis of PfCRT PL, as described in the following paper [18].

Supplementary Material

Refer to Web version on PubMed Central for supplementary material.

Acknowledgements

We thank our laboratory colleagues Jacqueline McCabe, Jacqueline Lekostaj, Changan Xie, and John Alumasa for experimental help. This work was supported by NIH grants AI045957 (PDR) and AI060792 (CW, PDR).

Supported by NIH grants AI045957 (P.D.R.) and AI060792 (C.W. & P.D.R.)

BIBLIOGRAPHY

1. Fidock DA, Nomura T, Talley AK, Cooper RA, Dzekunov SM, Ferdig MT, Ursos LM, Sidhu AB, Naude B, Deitsch KW, Su XZ, Wootton JC, Roepe PD, Wellems TE. Mutations in the *P. falciparum* digestive vacuole transmembrane protein PfCRT and evidence for their role in chloroquine resistance. Mol Cell 2000;6:861–871. [PubMed: 11090624]
2. Sanchez CP, McLean JE, Stein W, Lanzer M. Evidence for a substrate specific and inhibitable drug efflux system in chloroquine resistant *Plasmodium falciparum* strains. Biochemistry 2004;43:16365–16373. [PubMed: 15610031]
3. Sanchez CP, Rohrbach P, McLean JE, Fidock DA, Stein WD, Lanzer M. Differences in trans-stimulated chloroquine efflux kinetics are linked to PfCRT in *Plasmodium falciparum*. Mol Microbiol 2007;64:407–420. [PubMed: 17493125]
4. Zhang H, Paguio M, Roepe PD. The antimalarial drug resistance protein *Plasmodium falciparum* chloroquine resistance transporter binds chloroquine. Biochemistry 2004;43:8290–8296. [PubMed: 15222741]
5. Bray PG, Mungthin M, Hastings IM, Biagini GA, Saidu DK, Lakshmanan V, Johnson DJ, Hughes RH, Stocks PA, O'Neill PM, Fidock DA, Warhurst DC, Ward SA. PfCRT and the trans-vacuolar proton electrochemical gradient: regulating the access of chloroquine to ferriprotoporphyrin IX. Mol Microbiol 2006;62:238–251. [PubMed: 16956382]
6. Fitch CD. Chloroquine resistance in malaria: a deficiency of chloroquine binding. Proc Natl Acad Sci U S A 1969;64:1181–1187. [PubMed: 5271747]
7. Fitch CD. *Plasmodium falciparum* in owl monkeys: drug resistance and chloroquine binding capacity. Science 1970;169:289–290. [PubMed: 4988896]
8. Fitch CD, Yunis NG, Chevli R, Gonzalez Y. High-affinity accumulation of chloroquine by mouse erythrocytes infected with *Plasmodium berghei*. J Clin Invest 1974;54:24–33. [PubMed: 4600044]
9. Geary TG, Jensen JB, Ginsburg H. Uptake of [3H]chloroquine by drug-sensitive and -resistant strains of the human malaria parasite *Plasmodium falciparum*. Biochem Pharmacol 1986;35:3805–3812. [PubMed: 3535803]
10. Krogstad DJ, Gluzman IY, Kyle DE, Oduola AM, Martin SK, Milhous WK, Schlesinger PH. Efflux of chloroquine from *Plasmodium falciparum*: mechanism of chloroquine resistance. Science 1987;238:1283–1285. [PubMed: 3317830]
11. Bray PG, Howells RE, Ritchie GY, Ward SA. Rapid chloroquine efflux phenotype in both chloroquine-sensitive and chloroquine-resistant *Plasmodium falciparum*. A correlation of chloroquine sensitivity with energy-dependent drug accumulation. Biochem Pharmacol 1992;44:1317–1324. [PubMed: 1417955]
12. Martiney JA, Cerami A, Slater AF. Verapamil reversal of chloroquine resistance in the malaria parasite *Plasmodium falciparum* is specific for resistant parasites and independent of the weak base effect. J Biol Chem 1995;270:22393–22398. [PubMed: 7673225]

13. Sanchez CP, Wunsch S, Lanzer M. Identification of a chloroquine importer in *Plasmodium falciparum*. Differences in import kinetics are genetically linked with the chloroquine-resistant phenotype. J Biol Chem 1997;272:2652–2658. [PubMed: 9006900]

14. Bray PG, Janneh O, Raynes KJ, Mungthin M, Ginsburg H, Ward SA. Cellular uptake of chloroquine is dependent on binding to ferriprotoporphyrin IX and is independent of NHE activity in *Plasmodium falciparum*. J Cell Biol 1999;145:363–376. [PubMed: 10209030]

15. Lakshmanan V, Bray PG, Verdier-Pinard D, Johnson DJ, Horrocks P, Muhle RA, Alakpa GE, Hughes RH, Ward SA, Krogstad DJ, Sidhu AB, Fidock DA. A critical role for PfCRT K76T in *Plasmodium falciparum* verapamil-reversible chloroquine resistance. EMBO J 2005;24:2294–2305. [PubMed: 15944738]

16. Bray PG, Mungthin M, Ridley RG, Ward SA. Access to hematin: the basis of chloroquine resistance. Mol Pharmacol 1998;54:170–179. [PubMed: 9658203]

17. Gligorijevic B, Purdy K, Elliott DA, Cooper RA, Roepe PD. Stage independent chloroquine resistance and chloroquine toxicity revealed via spinning disk confocal microscopy. Mol Biochem Parasitol 2008;159:7–23. [PubMed: 18281110]

18. Paguio MF, Cabrera M, Roepe PD. Chloroquine Transport in *Plasmodium falciparum* II: Analysis of PfCRT Mediated Drug Transport Using Proteoliposomes and a Fluorescent Chloroquine Probe. Biochemistry, following paper this issue. 2009

19. Trager W, Jensen JB. Human malaria parasites in continuous culture. Science 1976;193:673–675. [PubMed: 781840]

20. Gligorijevic B, McAllister R, Urbach JS, Roepe PD. Spinning disk confocal microscopy of live, intraerythrocytic malarial parasites. 1. Quantification of hemozoin development for drug sensitive versus resistant malaria. Biochemistry 2006;45:12400–12410. [PubMed: 17029396]

21. Bennett TN, Paguio M, Gligorijevic B, Seudieu C, Kosar AD, Davidson E, Roepe PD. Novel, rapid, and inexpensive cell-based quantification of antimalarial drug efficacy. Antimicrob Agents Chemother 2004;48:1807–1810. [PubMed: 15105139]

22. Myers MC, Pokorski JK, Appella DH. Peptide nucleic acids with a flexible secondary amine in the backbone maintain oligonucleotide binding affinity. Org Lett 2004;6:4699–4702. [PubMed: 15575664]

23. Bennett TN, Kosar AD, Ursos LM, Dzekunov S, Singh Sidhu AB, Fidock DA, Roepe PD. Drug resistance-associated pfCRT mutations confer decreased *Plasmodium falciparum* digestive vacuolar pH. Mol Biochem Parasitol 2004;133:99–114. [PubMed: 14668017]

24. Dzekunov SM, Ursos LM, Roepe PD. Digestive vacuolar pH of intact intraerythrocytic *P. falciparum* either sensitive or resistant to chloroquine. Mol Biochem Parasitol 2000;110:107–124. [PubMed: 10989149]

25. Gligorijevic B, Bennett T, McAllister R, Urbach JS, Roepe PD. Spinning disk confocal microscopy of live, intraerythrocytic malarial parasites. 2. Altered vacuolar volume regulation in drug resistant malaria. Biochemistry 2006;45:12411–12423. [PubMed: 17029397]

26. Sullivan DJ Jr. Gluzman IY, Russell DG, Goldberg DE. On the molecular mechanism of chloroquine's antimalarial action. Proc Natl Acad Sci U S A 1996;93:11865–11870. [PubMed: 8876229]

27. Lekostaj JK, Natarajan JK, Paguio MF, Wolf C, Roepe PD. Photoaffinity labeling of the *Plasmodium falciparum* chloroquine resistance transporter with a novel perfluorophenylazido chloroquine. Biochemistry 2008;47:10394–10406. [PubMed: 18767816]

28. Leed A, DuBay K, Ursos LM, Sears D, De Dios AC, Roepe PD. Solution structures of antimalarial drug-heme complexes. Biochemistry 2002;41:10245–10255. [PubMed: 12162739]

29. Hayward R, Saliba KJ, Kirk KJ. The pH of the digestive vacuole of *Plasmodium falciparum* is not associated with chloroquine resistance. Cell Sci 2006;119:1016–1025.

30. Klonis N, Tan O, Jackson K, Goldberg D, Klemba M, Tilley L. Evaluation of pH during cytostomal endocytosis and vacuolar catabolism of haemoglobin in *Plasmodium falciparum*. Biochem J 2007;407:343–354. [PubMed: 17696875]

31. Kuhn Y, Rohrbach P, Lanzer M. Quantitative pH measurements in *Plasmodium falciparum*-infected erythrocytes using pHluorin. Cell Microbiol 2007;9:1004–1013. [PubMed: 17381432]

32. Reeves DC, Liebelt DA, Lakshmanan V, Roepe PD, Fidock DA, Akabas MH. Chloroquine-resistant isoforms of the *Plasmodium falciparum* chloroquine resistance transporter acidify lysosomal pH in

HEK293 cells more than chloroquine-sensitive isoforms. Mol Biochem Parasitol 2006;150:288–299. [PubMed: 17014918]

33. Naude B, Brzostowski JA, Kimmel AR, Wellems TE. *Dictyostelium discoideum* expresses a malaria chloroquine resistance mechanism upon transfection with mutant, but not wild-type, *Plasmodium falciparum* transporter PfCRT. J Biol Chem 2005;280:25596–25603. [PubMed: 15883156]
34. Ursos LM, DuBay KF, Roepe PD. Antimalarial drugs influence the pH dependent solubility of heme via apparent nucleation phenomena. Mol Biochem Parasitol 2001;112:11–17. [PubMed: 11166382]
35. Sidhu AB, Verdier-Pinard D, Fidock DA. Chloroquine resistance in *Plasmodium falciparum* malaria parasites conferred by pfcrt mutations. Science 2002;298:210–213. [PubMed: 12364805]
36. Ferrari V, Cutler DJ. Kinetics and Thermodynamics of chloroquine and hydroxychloroquine transport across the human erythrocyte membrane. Biochem Pharmacol 1991;41:23–30. [PubMed: 1986742]
37. Casabianca LB, An D, Natarajan JK, Alumasa JN, Roepe PD, Wolf C, de Dios AC. Quinine and chloroquine differentially perturb heme monomer-dimer equilibrium. Inorg Chem 2008;47:6077–6081. [PubMed: 18533646]
38. Casabianca LB, Kallgren JB, Natarajan JK, Alumasa JN, Roepe PD, Wolf C, de Dios AC. Antimalarial drugs and heme in detergent micelles: An NMR study. J Inorg Biochem 2009;103:745–748. [PubMed: 19223262]

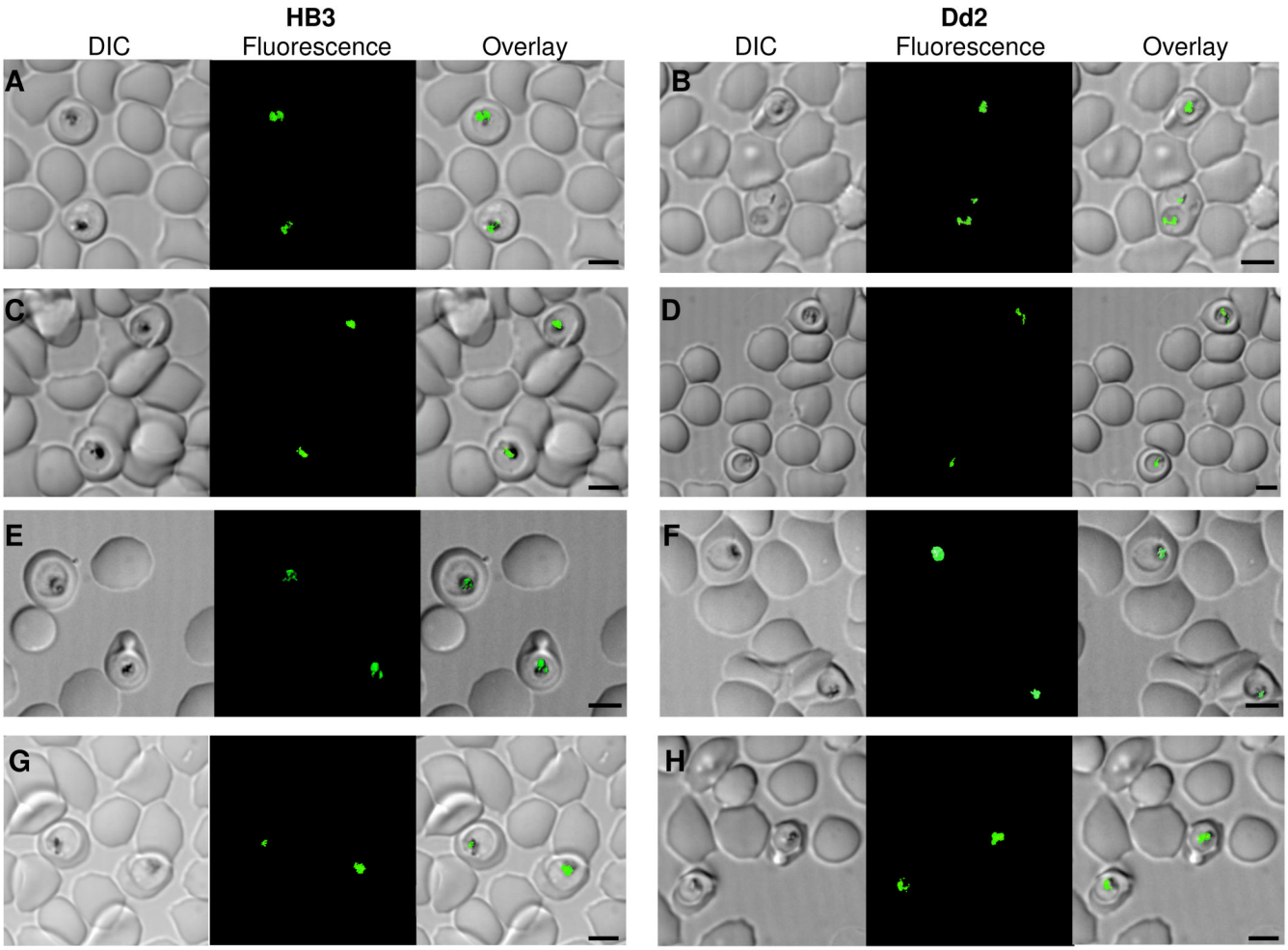

Figure 1. Localization of NBD-CQ in the digestive vacuole of *Plasmodium falciparum* using SDCM

DIC (left), fluorescence (middle), and DIC with fluorescence overlay images of a single optical Z-section of late trophozoite stage CQS HB3 (A, C, E, G) or CQR Dd2 (B, D, F, H) parasites in intact iRBCs, perfused with 250 nM NBD-CQ in gas balanced HBSS. (A, B) 250 nM NBD-CQ in normal HBSS that contains 5 mM D-Glucose. (C, D) ATP depleted conditions with 250 nM NBD-CQ in HBSS and 2 mM 2-Deoxy-D-glucose in place of 5 mM D-Glucose. (E, F) 250 nM NBD-CQ in HBSS without glucose. (G, H) 250 nM NBD-CQ in HBSS with glucose and 1 uM verapamil. The scale bar in each set of panels = 4.0 μm.

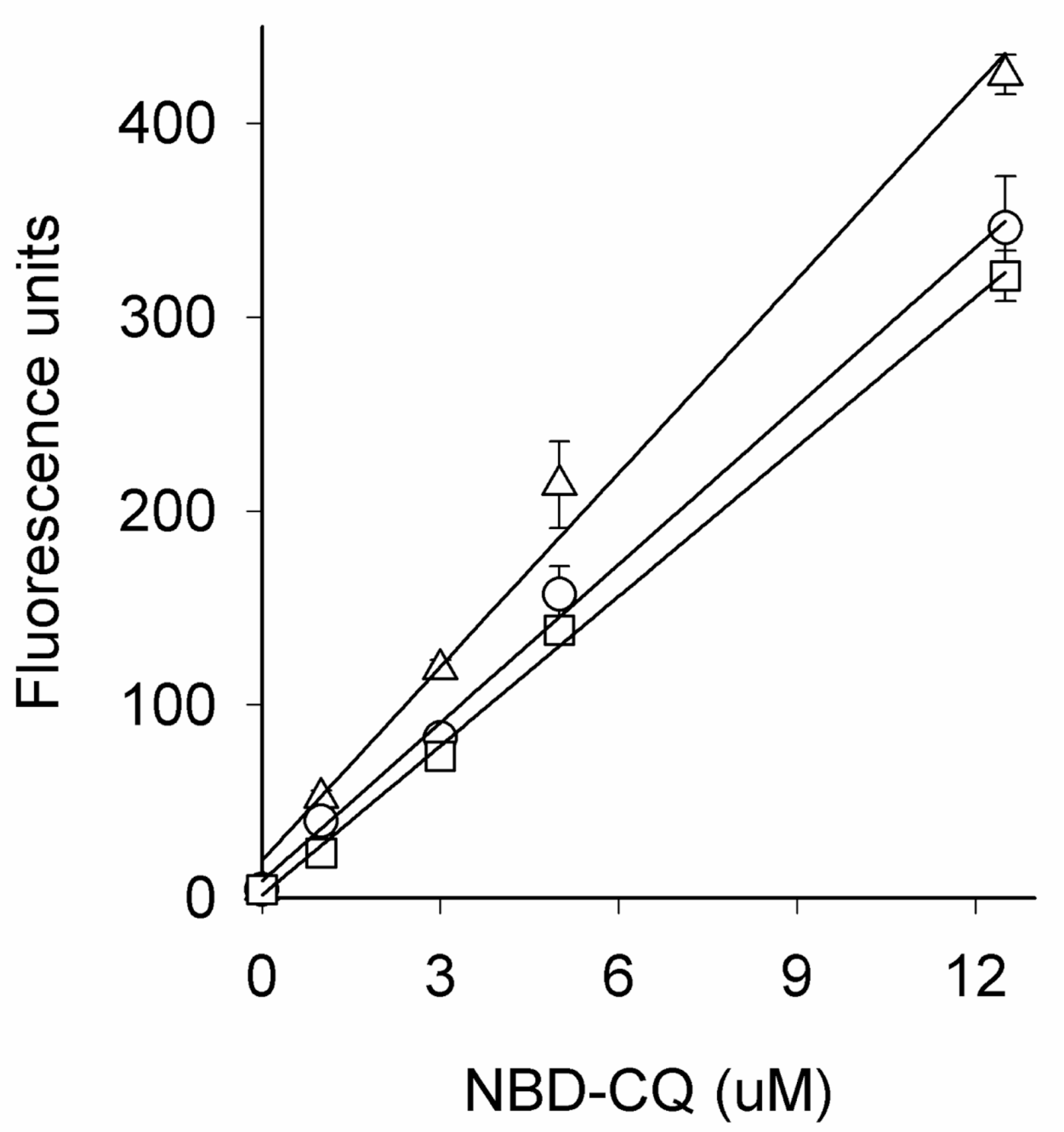

Figure 2.
NBD-CQ fluorescence measured via thin layer calibration methods (see [24]) in the presence of 100 nM heme (○), 1 μM heme (□), or no heme (Δ). Heme solutions were prepared from 5 mM hematin dissolved in 0.1 M NaOH, titrated to pH 5.5, and then added to different concentrations of NBD-CQ dissolved in 50 mM MES-Tris pH 5.5.

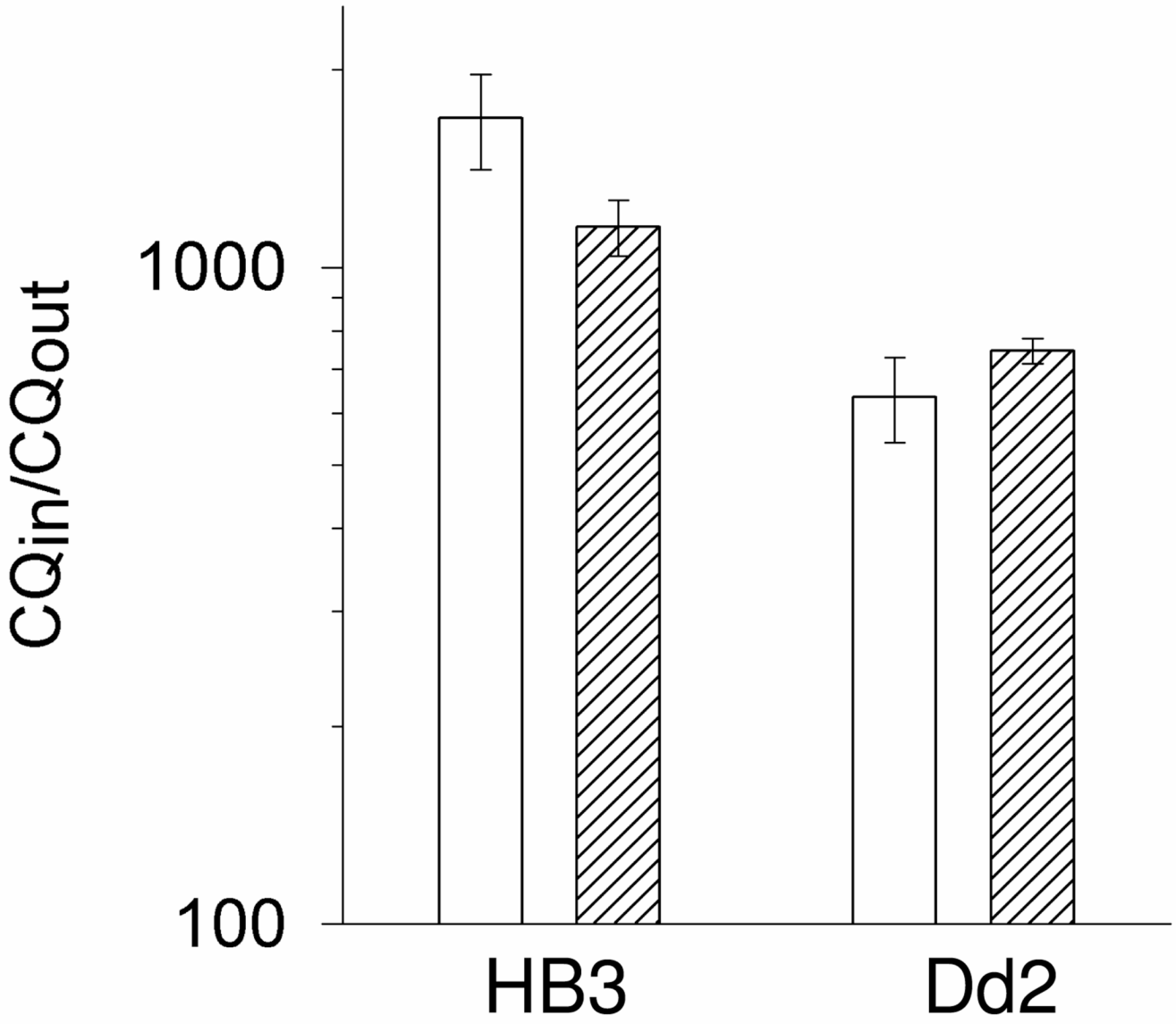

Figure 3. ^{3}H-CQ and NBD–CQ accumulation in iRBC

HB3 and Dd2 iRBC were incubated with 1 nM ^{3}H-CQ (open bars) or 1 nM NBD-CQ (hashed bars) as described in the Methods. Accumulation was measured as the ratio of the concentration of the probe inside the iRBC vs. the concentration of the external incubating probe concentration and is presented on a log scale. Error bars were calculated from the standard error of the mean (SEM). *Note* that unlike many other studies in the past 10 years, we do not subtract theoretical calculated “non saturable” uptake from these data. These represent raw unprocessed differences for CQS vs. CQR net accumulation.

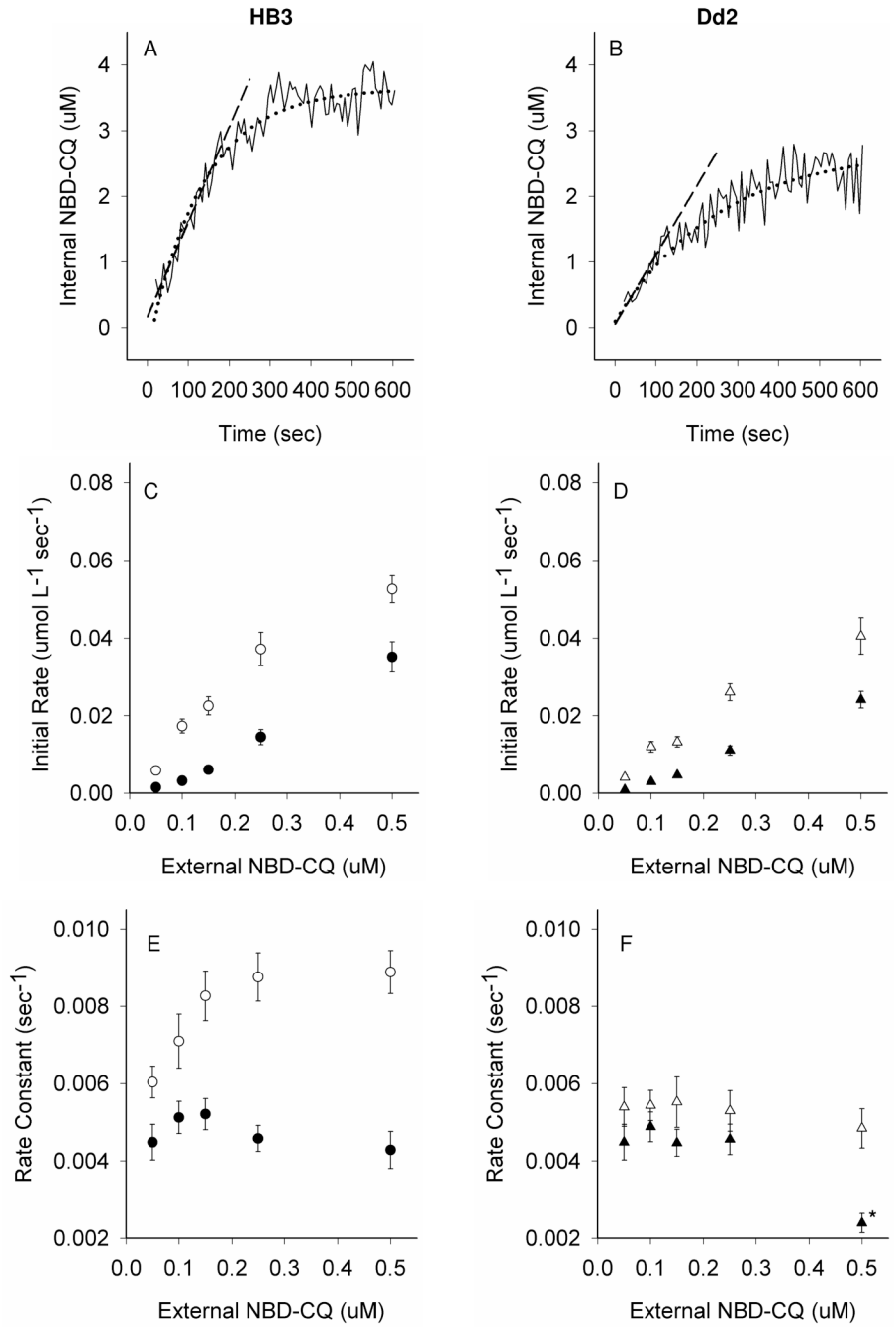

Figure 4. NBD–CQ influx under continuous perfusion

(A, B) Representative accumulation traces and illustration of curve-fitting methods for 100 nM NBD-CQ influx in CQS HB3 (A) or CQR Dd2 (B) parasites under continuous perfusion with NBD-CQ as described in the text. Solid black lines show the raw data; accumulation (internal NBD-CQ on the y-axis) vs. time under perfusion with constant 100 nM NBD– CQ (x-axis). Black dashed lines represent linear curve fits to the first 60 sec (apparent initial rate) using $y = mx + b$. Black dotted lines show exponential curve fits for rate constant determinations using $f = y_o + a(1\text{-}e^{-bx})$, where the rate constant is "b". Initial rates (C, D) and rate constants of influx (E, F) at various external NBD-CQ concentrations were measured in gas balanced HBSS with 5 mM D-Glucose (open symbols) vs. 5 mM D-Glucose substituted with 2 mM 2-Deoxy-D-

glucose (filled symbols). (C) HB3 initial rates of influx with (○) and without glucose (●). (D) Dd2 initial rates of influx with (Δ) and without glucose (▲). (E) HB3 rate constants for influx with (○) and without glucose (●). (F) Dd2 rate constants for influx with (Δ) and without glucose (▲). Each point is the average of >20 parasites from at least 5 independent perfusion experiments. All error bars were calculated from the standard error of the mean (SEM). One set of experimental conditions for Dd2 (marked with *) repeatedly led to ambiguous rate constant calculation since, despite many attempts, the accumulation traces in these experiments did not provide a clear plateau within 15–20 minutes. This phenomenon (seen only at higher [NBD-CQ]) will be explored elsewhere.

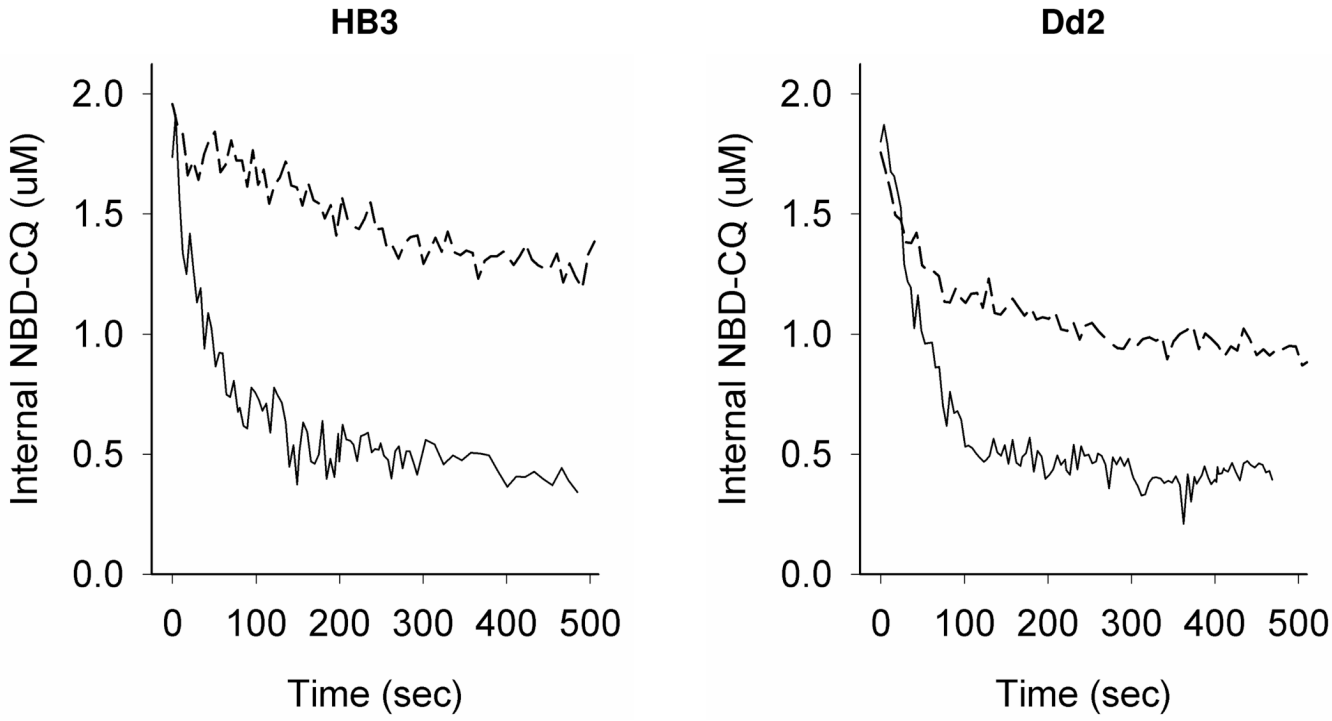

Figure 5. NBD – CQ efflux in live intraerythrocytic *P. falciparum*

Shown are representative traces for NBD-CQ efflux from live CQS HB3 (left) and CQR Dd2 (right) parasites. Preloading conditions were by incubation of low inoculum iRBC with 30 or 50 nM NBD-CQ (for HB3 or Dd2, respectively) in HBS for 1 hr (top trace, each panel) and with 250 or 500 nM NBD-CQ (for HB3 or Dd2, respectively) for 1 min under perfusion with HBSS (bottom trace each panel). The incubating concentrations were chosen such that total internal probe would be equivalent for both the CQS and CQR strain. For cells pre-loaded with NBD-CQ for 1 hr, efflux was initiated by perfusion with HBS at 37 °C (top trace each panel, broken line) similar to many previous studies. For cells preloaded via a short pulse with NBD-CQ, efflux was initiated by immediately switching to HBSS (bottom trace each panel, solid lines).

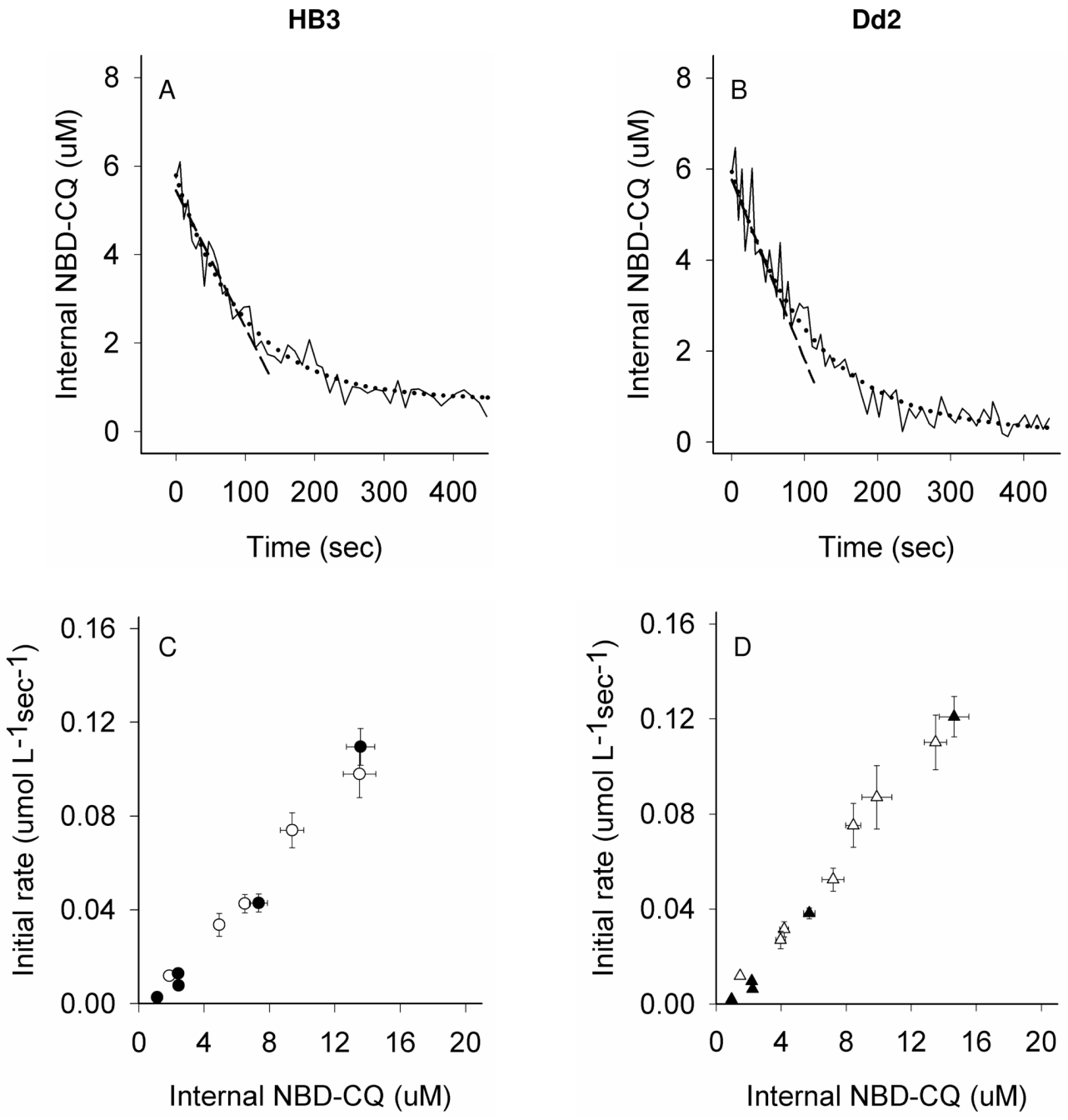

Figure 6. NBD–CQ efflux under continuous perfusion

Shown are representative NBD-CQ efflux traces for CQS HB3 (A) and CQR Dd2 (B) parasites. Efflux data under continuous perfusion conditions was obtained after the parasites had accumulated NBD-CQ via perfusion with gas balanced HBSS for 15 min (as shown in Fig. 3 A,B). The zero time point for efflux is the internal NBD-CQ concentration immediately before perfusate is switched to gas balanced HBSS without NBD-CQ. The solid black lines are the raw data; NBD–CQ efflux traces (internal NBD-CQ on the y-axis) vs. time under perfusion (x-axis); the black dashed lines represent linear curve fits to the first 60 sec for initial rate determination using $y = mx + b$ and black dotted lines show exponential curve fits for rate constant determinations using $f = y_o + ae^{-bx}$. For parasites with varying internal NBD-CQ

concentrations after 15 min of accumulation with varying external, the initial rates of efflux were measured under continuous perfusion with gas balanced HBSS either in the presence (open symbols) or the absence (closed) of glucose, for CQS HB3 (panel C) and Dd2 (panel D). (C,D) Straight line fits to these initial rate plots (not shown) obtained in the presence of glucose give a slope of 7.6×10^{-3} for HB3 and 8.7×10^{-3} for Dd2. In the absence of glucose, the slopes of these plots (not shown) are 7.2×10^{-3} for HB3 and 8.9×10^{-3} for Dd2, consistent with larger amplitude in efflux for CQR Dd2 parasites that increases as internal [probe] increases.

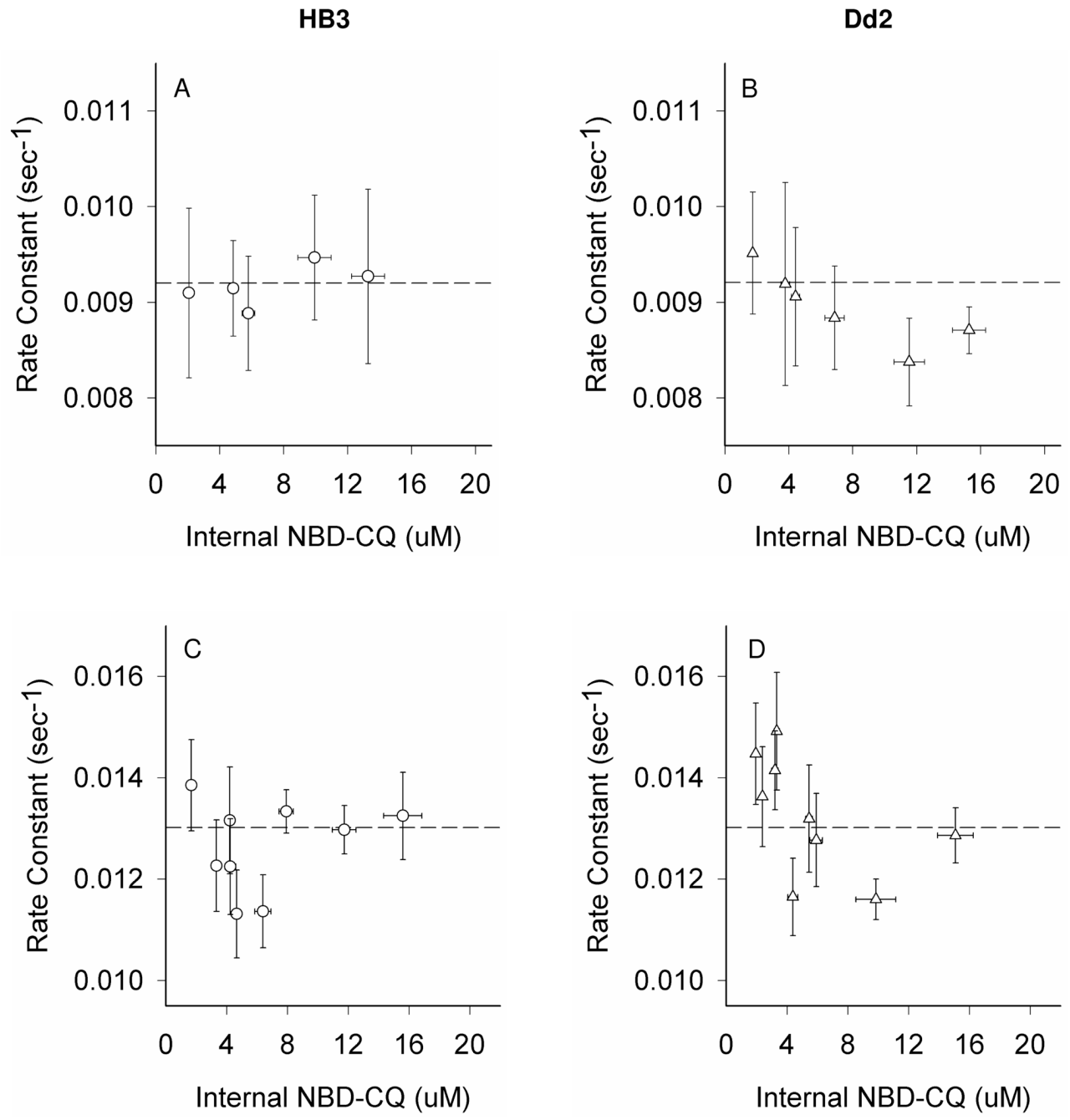

Figure 7. Rate constants for zero trans NBD–CQ efflux under continuous perfusion

Zero trans efflux rate constants were measured for parasites preloaded with NBD-CQ in gas balanced HBSS. Preloading accumulation of NBD-CQ was 15 min of continuous perfusion (A,B) or 1 min perfusion (C,D) with varying NBD-CQ concentrations needed to attain similar initial DV concentrations (x axis). Each point is the average of >20 parasites from at least 5 independent perfusion experiments. All error bars (x,y) were calculated from the standard error of the mean (SEM). Dashed lines are positioned at the same Y axis value for A,B and C,D for visual reference.

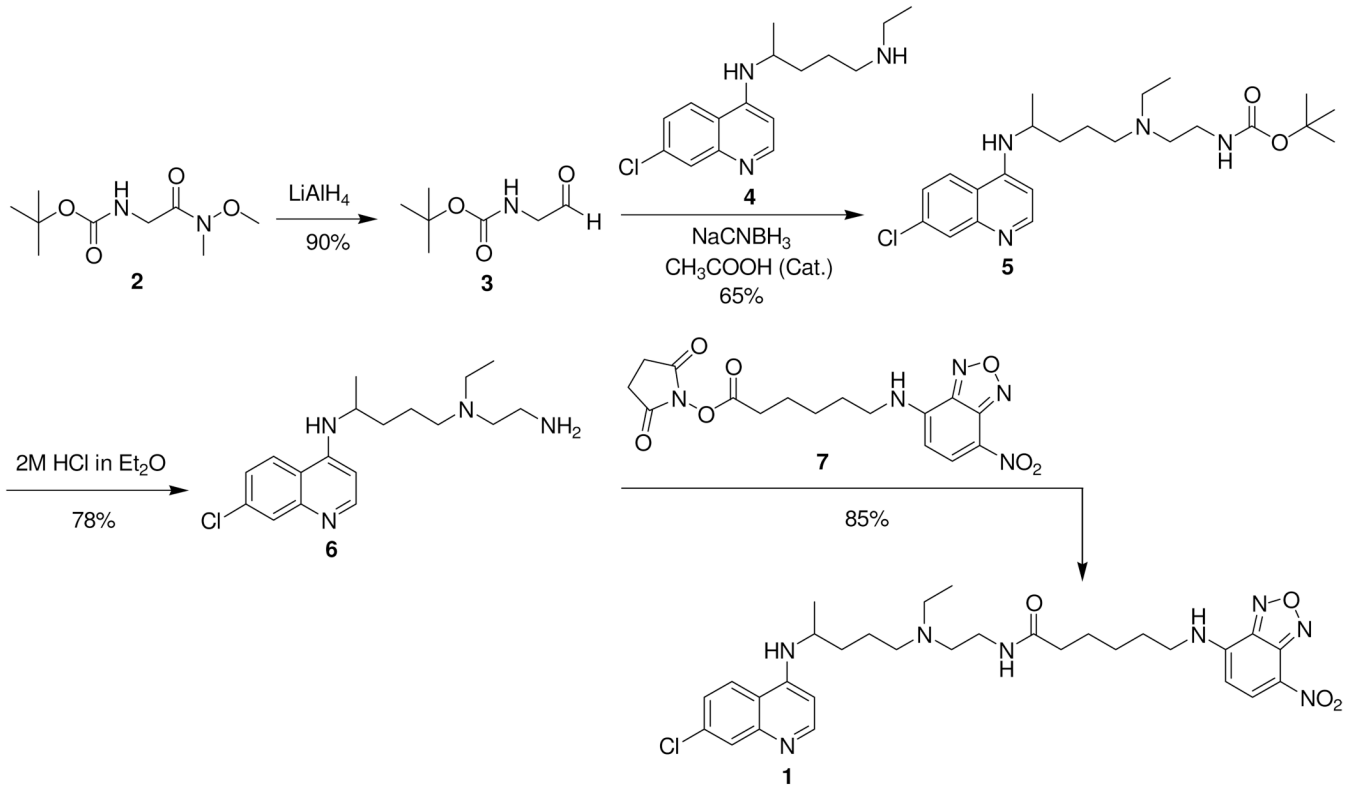

Scheme 1.

Table 1

DV NBD-CQ Concentration.

External NBD-CQ (μM)	Internal NBD-CQ (μM)[a]	
	HB3	Dd2
0.050	1.86 ± 0.11	1.47 ± 0.07
0.10	4.92 ± 0.25	3.96 ± 0.30
0.15	6.48 ± 0.34	4.17 ± 0.27
0.25	10.6 ± 1.0	8.20 ± 0.67
0.50	14.1 ± 1.0	9.87 ± 0.92

[a]The mean of the internal NBD-CQ concentrations for individual HB3 and Dd2 parasites in intact iRBCs were determined after 15 min of perfusion with different known NBD-CQ concentrations in gas balanced HBSS. Internal concentrations were obtained from thin layer calibration curves (see Fig. S5) and influx traces as shown in Fig. 4, A and B.

Table 2

Summary of Accumulation Kinetics at 250 nM NBD-CQ external concentration.

	DV Internal concentration at plateau[a] (μM)		
Glucose*	+	–#	+
VPL^	–	–	+
HB3	10.6 ± 1.0	8.20 ± 0.94	9.99 ± 0.46
Dd2	7.33 ± 0.72	10.8 ± 0.74	8.95 ± 0.5
$C2^{GCO3}$	9.81 ± 0.56	8.26 ± 0.64	10.1 ± 0.76
$C4^{Dd2}$	7.91 ± 0.56	10.8 ± 1.0	9.98 ± 0.73
	Initial Rates ($\mu mol\ L^{-1} sec^{-1} \times 10^{-2}$)		
Glucose*	+	–#	+
VPL^	–	–	+
HB3	4.24 ± 0.47	2.22 ± 0.35	4.94 ± 0.35
Dd2	2.61 ± 0.22	3.23 ± 0.34	3.48 ± 0.27
$C2^{GCO3}$	3.90 ± 0.32	1.56 ± 0.22	4.69 ± 0.51
$C4^{Dd2}$	2.37 ± 0.17	2.55 ± 0.44	3.61 ± 0.32
	Rate Constants ($sec^{-1} \times 10^{-3}$)		
Glucose*	+	–#	+
VPL^	–	–	+
HB3	8.03 ± 0.63	4.43 ± 0.25	9.85 ± 0.61
Dd2	5.29 ± 0.53	4.63 ± 0.39	7.21 ± 0.76
$C2^{GCO3}$	7.05 ± 0.33	3.42 ± 0.37	9.43 ± 0.65
$C4^{Dd2}$	4.24 ± 0.32	3.91 ± 0.30	8.51 ± 0.83

*5mM D-Glucose

#No glucose substitution

^1μM Verapamil

[a]Using external 250 nM NBD-CQ, influx kinetics were measured in the presence (2^{nd} column), vs absence of glucose (3^{rd} column) and with a constant external concentration of 1 μM Verapamil (4^{th} column) for several parasite lines; CQS parasites HB3 and $C2^{GCO3}$, and CQR parasites Dd2 and $C4^{Dd2}$. Similar patterns were also measured at 100 and 500 nM NBD-CQ in the perfusate (data not shown).